On the Potential of Zeotropic Mixtures in Supercritical ORC Powered by Geothermal Energy Source

Jovana Radulovic[a*], Nadia I. Beleno C.[a]

[a] School of Engineering, University of Portsmouth, Portsmouth PO1 3DJ, UK

Abstract

Six zeotropic mixtures are proposed for conducting a parametric optimisation of supercritical Rankine cycle powered by low temperature geothermal heat source. Different mixing ratios of two types of zeotropic mixtures were studied and their performance evaluated in the range of process parameters. Optimal operational conditions were identified for each mixture and their advantages over pure fluids quantified. The results indicate that the choice of pressure and temperature at the turbine inlet can be tuned to the mixture properties. Thermal and exergy efficiencies of R-143a/R-124 mixtures were higher than for R-143a/R-C318 mixtures in the range of process parameters studied. Mixture R-143a(0.2)/R-124(0.8) yielded the highest thermal efficiency of 16% at evaporator pressure value of 10 MPa and maximum operational temperature 470 K. The highest exergetic efficiency of 47% was developed by R-143a(0.7)/R-124(0.3) at 3.9 MPa and 365 K. A comparative analysis between the zeotropic mixtures and pure R-143a shows that the cycle efficiency can be improved by 15% at the same operational conditions.

[*] Corresponding author: Address: School of Engineering, University of Portsmouth, Anglesea building, PO1 3DJ Portsmouth, UK.
Telephone: +44 (0)23 9284 2113. E-mail: Jovana.Radulovic@port.ac.uk

Graphical abstract

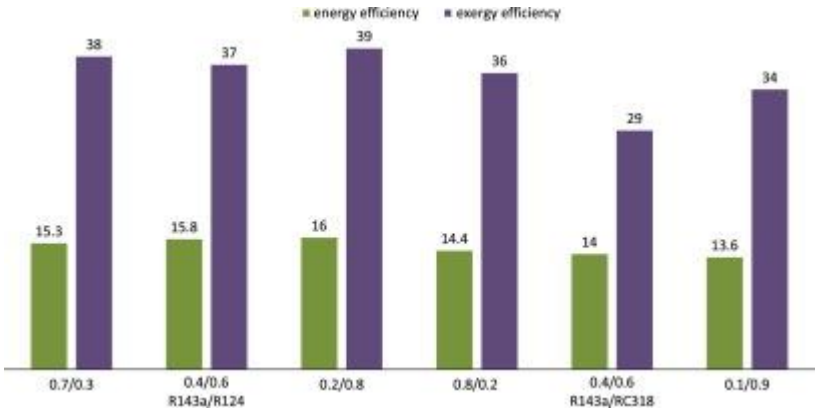

Nomenclature

Symbols

EDF	exergy destruction factor
h	specific enthalpy (kJ/kg)
p	pressure (MPa)
s	specific entropy (kJ/kgK)
T	temperature (K)
η	thermal efficiency
η_{II}	exergy efficiency

Subscript

0	ambient condition
1,2,3.etc.	state points of the SRC system

b	boiler
c	condenser
p	pump
t	turbine

1. Introduction

Over the last decades the methods used to produce electric energy have been highly revised. Renewable energies like solar, wind, biomass or geothermal are widely used nowadays, while development of novel and more efficient energy systems continue to be in focus of current research investigations. Organic Rankine Cycle (ORC) is one of the promising technologies as it allows for the use of the low temperature heat sources, typically below 300°C. ORC research has been concentrated on improving the efficiency through more rigorous selection of the working fluid, but also on alterations of the cycle design (Karellas and Schuster, 2008, Papadopoulos et al., 2010, Schuster et al., 2010). In general, three types of ORC for low grade heat have been studied: subcritical, supercritical and transcritical. Subcritical and transcritical cycles have been mostly investigated for low-temperature geothermal power (Shengjun et al., 2011). However, promising higher efficiencies can be achieved with supercritical approach as Shuster et al. (Schuster et al., 2010) pointed out. Saleh et al. (Saleh et al., 2007) performed a comprehensive analysis which included 31 pure components. The authors assessed the performance of working fluids under both subcritical and supercritical conditions and reported noticeable differences in thermal efficiencies: R-143a reached thermal efficiency of 7.5% in subcritical conditions whereas working at supercritical conditions developed up to 9.3%. Their research concluded that supercritical cycles with appropriately chosen substances, such as R-

143a, show similar thermal efficiencies (about 9%) and similar low volume ratios as the subcritical cycles of fluids like R-152a. Shortly after, Schuster et al. (Schuster et al., 2010) demonstrated that the maximum thermal efficiency of supercritical cycles was 14.4% compared with 13.3% for subcritical state. Similarly, Karellas and Schuster (Karellas and Schuster, 2008) conducted a study of supercritical parameters. However, the fluids they tested were limited to R-245fa and R-227ea/R-134a in different ORC applications powered by waste heat and geothermal, respectively. Tchanche et al. (Tchanche et al., 2009) also pointed out the importance of working with supercritical organic Rankine cycles and its possible advantages due to potentially good performance.

Angelino and Di Paliano (Angelino and Colonna di Paliano, 1998) explored the idea of using a mixture of fluids for high performance in high and low grade heat ORC instead of pure fluids. Their comparison showed the advantages of non-isothermal phase change of the mixture and revealed the possibility to select the mixture for a specific application depending on nature of the mixture (wet or dry) and the number of constituents. Wang and Zhao (Wang and Zhao, 2009) performed the analysis of zeotropic mixtures for low grade heat (solar applications) ORC. They investigated a single mixture of R-245fa (dry fluid) and R-152a (wet fluid) with three different mass fractions (0.9/0.1; 0.65/0.55; 0.45/0.55) in the range of temperatures between 25°C and 85°C; the intermediate mixture composition exhibited isentropic saturated vapour line. By analysing the two factors, efficiency and volume flow rate, as Saleh et al. (Saleh et al., 2007) did, it was concluded that despite the higher Rankine cycle efficiency achieved by pure R-245fa, a zeotropic mixture showed a lower volume ratio; hence larger dimensions and more expensive expander for pure R-245fa. Another important finding is that Rankine efficiency for isentropic zeotropic mixture was lower than for dry and wet mixture.

Zeotropic mixtures received significant scientific attention in recent years (Zhao and Bao, 2014, Dong et al., 2014). Heberle et al. (Heberle et al., 2012) studied isobutene/isopentane and R-227ea/R-245fa mixtures, while Chen et al. (Chen et al., 2011) introduced the idea of zeotropic mixtures working at supercritical conditions. They conducted the analysis based on a mixture of R-134 and R-32 (0.7/0.3 mass fraction) and compared the performance of the mixture with the pure fluid working at subcritical conditions. Moreover, in their study they listed 22 fluids as potential candidates for composing zeotropic mixtures taking into account their environmental impact and thermodynamic properties.

Several reviews (Chen et al., 2010, Bao and Zhao, 2013) shed light on the necessity to conduct further research in the domain of selection of suitable working fluid, especially when fluid mixtures are employed in supercritical Rankine cycle (SRC). In this study we addressed one of the most important areas of contemporary engineering, which is the production of the electric power more efficiently and with a minimal impact to the environment. We studied the behaviour of selected zeotropic mixtures in SRC and assessed their potential as working fluids. The optimal operational parameters were identified through calculated energy and exergy efficiencies.

2. Cycle configuration and optimisation method

2.1. Cycle configuration

Figure 1(a) shows the standard layout of a simple cycle. The working fluid goes along the loop through four fundamental processes that involve pressure and temperature changes. Saturated

liquid at low pressure and the minimal temperature conditions is pumped above its critical pressure by the feed pump (process 1 – 2). Heat from a low temperature source is supplied to the working fluid (process 2 – 3), after which the supercritical fluid is expanded through a turbine to the condenser pressure (process 3 – 4). Finally, the heat is rejected from the superheated or saturated vapour until saturated liquid state is reached (process 4 – 1).

2.2. Heat source and assumptions

The process was simulated assuming geothermal energy as a primary heat source; however, biomass and waste heat can also be considered. Our model is based on low-grade heat source with temperature range between 360 K and 480 K. Only supercritical conditions were considered in this study. The maximum pressure value was initially not capped since it is one of the crucial optimization parameters. However, restrictions in terms of manufacturing and maintenance were taken in account and are discussed in following sections. Parametric analysis is based on a steady state operation. Pressure drop in pipes and heat losses to the environment in all cycle elements are neglected. The condenser outlet state is saturated liquid, which is assumed to be at the temperature approximately 10°C higher than that of the cooling fluid. Similarly, at the boiler/vapour generator inlet working fluid is modelled as subcooled liquid at supercritical pressures and at approximately 10°C lower temperature than the heat source. These and other assumptions summarised in Table 1 are based on the typical values found in the literature; see (Wang et al., 2014) and references therein.

120

121 *2.3. Zeotropic mixture – working fluid selection process*

122

123 Zeotropic mixture is characterised by unequal concentrations of the liquid and the vapour
124 phase. During the phase change this property of the mixture causes a temperature glide. Unlike
125 azeotropic mixture, *T-h* diagram of a zeotropic one shows prominent non-linearity
126 (Radermacher and Hwang, 2005). For synthesizing zeotropic mixtures we have considered the
127 chemical compounds deemed suitable by Chen et al. (Chen et al., 2011, Chen et al., 2010).
128 Additionally, thermodynamic properties, stability and compatibility with the cycle materials,
129 environmental and safety concerns were also taken in account. Substances R-143a, R-218, R-
130 125, R-41, R-170 and CO_2 have been already tested under supercritical conditions; the highest
131 thermal efficiency of the cycle was reached when R-143a, R-170 and R-218 were employed
132 (Saleh et al., 2007). In addition, zeotropic mixture of R-32 and R-134a has been analysed at
133 supercritical conditions (Chen et al., 2010).

134

135 Given that R-143a fluid achieved the best performance in terms of thermal efficiency (Chen et
136 al., 2010), it has been chosen as a common component for the synthesis of zeotropic mixtures
137 studied. Since it is a wet fluid, it is desirable for the second component to be either isentropic
138 or dry in order to produce a mixture with a convenient saturated vapour line (Figure 1b). In
139 general, dry and isentropic organic working fluids with positive and nearly infinitely large slopes
140 (*dT/ds*), respectively, are the ones that provide better ORC performance (Hipólito-Valencia et
141 al., 2013). The second element of the mixture was selected from 22 short-listed compounds
142 presented in (Chen et al., 2011). Taking into account both hard (toxicity, stability, ODP and

143 critical point) and soft criteria (flammability, other thermodynamic properties and availability)
144 R-124 was chosen as the isentropic and R-C318 as a dry fluid.
145
146 Once the components were selected, the temperature glide of the binary mixtures was
147 evaluated to determine the mole fractions of individual constituents within the mixture that
148 can best match with the heat exchanging fluid in the condensation process. Molar fractions that
149 allow for glide temperatures variation of more than 5 K and less than 15 K were considered in
150 the calculations as suggested by Herberle et al. (Heberle et al., 2012). After the analysis of the
151 glide temperature (Figure 2) six zeotropic mixtures, summarised in Table 2, were selected. One
152 of the compositions for each mixture was taken for the peak glide temperature, whereas the
153 other two were selected in such manner to have relatively similar temperature glide values, yet
154 different compositions in order to study how dominance of a particular component in the
155 mixture affects the cycle performance.
156
157 *2.4. Operating conditions*
158
159 The minimum pressure at point 3 was obtained from the REFPROP database 23 software where
160 the critical properties were calculated using the Helmholtz free energy equation (NIST standard
161 reference database 23, NIST thermodynamic and transport properties of refrigerant and
162 refrigerant mixtures REFPROP, National Institute of Standards and Technology of the United
163 States). For each mixture and composition, the critical pressure and temperature were
164 determined and the operational parameters were tailored to assure the supercritical state of
165 the working fluids at the turbine inlet (Table 3). The assumed ΔT = 10°C between the cold and
166 the hot fluid in the condenser ensures low complexity and sensible size of the heat exchanger.

167 The average air temperature being approximately 15°C implies that, according to the above
168 assumption, the temperature of the mixture at the turbine outlet is 25°C. This value was then
169 used to determine the condensation pressure, also given in Table 3.

170

171 *2.5. Optimisation method*

172

173 Sink conditions stated above are kept constant during the optimization process, as well as the
174 other assumptions discussed previously. Computations were performed by changing the high
175 pressure of the cycle with the rise of the turbine inlet temperature in order to find the pressure
176 range which gives the maximum thermal efficiency. Therefore, increasing the high pressure was
177 matched by necessary rise in the maximum cycle temperature to ensure cycle operation are
178 supercritical conditions. The other requirement - the minimum vapour quality at the turbine
179 exit of 90% was maintained in all our calculations. Calculated thermal efficiency of the SRC for
180 selected mixtures, based on the two conditions specified above, is presented as a function of
181 the increasing turbine inlet pressure in Figure 3. Starting from the minimum (critical) pressure,
182 stated in Table 2, increase of pressure led to the rise of thermal efficiency of SRC as expected.
183 Efficiency values increase rapidly until the maximum is reached, after which they start to
184 monotonically decrease. This trend was more prominent for R-143a/R-124 mixtures, which also
185 had higher thermal efficiencies in general. It is worth mentioning that for R-143a/R-C318
186 mixtures increase in thermal efficiency was proportional to the molar fraction of R-143a in the
187 mixture, while for R-143a/R-124 mixtures this was not the case at very high pressure levels
188 indicating that the nature of interactions between the mixture components is very sensitive to
189 drastic pressure changes.

For all selected mixtures the maximum thermal efficiencies were reached within a pressure range of 8 to 16 MPa. While the optimisation of the high pressure level has the purpose to identify potential for improvement of the SRC and achieve more efficient energy utilisation within the cycle, we proceeded with the modelling considering high pressure values between the minimum one specified for each supercritical mixture and 10 MPa. The maximum pressure of 10 MPa is a realistic and manageable parameter that takes in account the limitation and the cost of manufacture as well as the design of the turbine (Kaşka, 2014). Apart from the turbine inlet pressure this study is also focused on the effect of the other key parameter - turbine inlet temperature (TIT) on the thermal and exergetic efficiency. The initial conditions for TIT were set according to the supercritical parameters of each mixture and the source temperature was varied to the maximum available value. The properties at each state were obtain from REFPROP database 23 software; the energy and exergy analysis was performed for the six different mixtures under the conditions stated above.

3. Optimisation results and analysis

3.1. Energy analysis

The computed thermal efficiencies of the supercritical Rankine cycle for six zeotropic mixtures under their optimised working parameters are shown in Figure 4. Naturally, the maximum thermal efficiency was achieved at the maximum selected pressure and the highest heat source temperature (10 MPa and 480 K). In the range of investigated cycle parameters higher thermal efficiencies were found for the first three mixtures. In particular, M3 (R-143a(0.2)/R-124a(0.8)

exhibited the highest performance with a 16% of energy efficiency at 9 MPa and 470 K at the entrance to the turbine. These results suggest that the R-143a/R-124 combination is a better thermodynamic match, as a poorer chemical synergy is observed between a wet and a dry fluid. While the decrease in wet fluid concentration caused a drop in thermal efficiency for R-143a/R-C318 mixtures, the opposite was observed for R-143a/R-124 mixtures. Isentropic fluids have been recognised as ideal working fluids in ORC (Bao and Zhao, 2013) and higher proportion of R-124 in the mixture leads to better performance.

In order to augment the thermal efficiency of the cycle the heat input is to be minimised while achieving the highest possible work output from the heat supplied. Figure 5 shows that, alike thermal efficiencies, lower work outputs were found for R-143a/R-C318 mixtures. Higher net work observed for the other set of zeotropic mixtures, R-143a/R-124, needed larger heat input. The mixture with the highest thermal efficiency, M3, neither required the lowest heat input nor achieved the highest work output; it attained an efficient balance between the two. In addition, it is clear the high heat input can be directly related to the high proportion of the first component in the mixture. However, larger amount of R-143a also lead to higher work outputs. As the concentration of the second component in the mixture increases the heat intensity needed to reach TIT of 470 K decreases. This is due to differences in the specific heat as well as variations in vapour generator inlet temperature. The specific heat of the first component (R-143a) is higher than those for the other two components. Therefore, we observe a drop in the specific heat of the mixture as the amount of the second components increases; the overall heat input decreases and the work output as well. In addition to the specific heat, the glide temperature also has an impact on the pump output temperature and therefore, has an effect on the heat needed in the vapour generator. The pump output temperature (state 2) decreases

significantly in mixtures M2 and M5, which are the compositions that present the maximum temperature glide in the condensation process (11 K and 14.3 K, respectively). Consequently, the temperature range during the heat addition process is narrowed. Yet, mixture M3 appears to have desirable intrinsic properties to aid in the heat input reduction; its specific heat and the glide temperature allow for the use of low-temperature source to power the cycle.

Figure 6 shows the comparisons between the specific turbine work output and pump work input for the six zeotropic mixtures analysed at optimised parameters. For both types of zeotropic mixtures high work inputs and outputs were observed for mixtures in which the dominant component was R-143a. The work out/work in ratio was found to be larger for M1-M3 mixtures, mostly due to greater work of the expansion in the turbine. The highest value of 5.5 was calculated for M3. It is worth mentioning that this ratio was also directly increasing with the concentration of the second component for the M1-M3. Out/in work ratio varied less for second set of mixtures, M4-M6, and without a trend that can be clearly related to the relative mixture concentrations; the highest value was found for M5 (4.6).

Work of the pump depends on both the lower and higher pressure of the cycle as well as on the density of the working fluid. The lower pressure is dictated by the condensation temperature, which was fixed at 298 K. Optimised high and low values of operational pressures for the six mixtures analysed in this study are given in Tables 4 and 3, respectively. As the concentration of the second component increases, the saturation line changes from wet to isentropic or dry, and consequently the lower pressure (saturation vapour pressure) decreases. Although the ΔP increases when the amount of second component in the mixture increases, the pump work required to reach this pressure decreases due to the differences in densities

between the mixtures. The specific volume is lower with more second component in the mixture increases as they both have higher densities than the first one.

3.2. Exergy analysis

Exergy analysis was carried out to estimate exergy destruction in each component of the cycle, as well as to assess the effect of optimised turbine inlet temperature and pressure on exergy performance. The second law efficiency was calculated according to Equations 1 and 2.

$$\frac{1}{\eta_{II}} = 1 + Total \quad exergy \quad destruction \quad factor \tag{1}$$

$$Total \quad EDF = EDF_{boiler} + EDF_{condenser} + EDF_{pump} + EDF_{turbine} \tag{2}$$

The maximum exergetic efficiency for each mixture at their optimised parameters is shown in Figure 7. Higher exergy efficiencies were calculated for R-143a/R-124 mixtures, with maximum values of 47.4% and 47.0% found for M1 and M3, respectively. Intermediate mixture compositions had lower exergy efficiencies. In general, higher second law efficiency values can be attributed to R-143a-rich mixtures. When comparing these results with the total exergy destroyed in the cycle (Figure 8), it can be seen that the mixture with the highest exergetic efficiency was not the one with least irreversibilities. The optimal selection of a mixture would be the one with the best balance between the exergy destroyed and the exergy recovered from

the heat source. The latter varies amongst the mixtures: it increases with the amount of the second component for mixtures M1-M3, whilst for M4-M6 it reaches a peak for M5. Despite M4 having the lowest exergy destroyed, it also has lower exergy recovered from the heat source. It is worth noting that optimal exergetic conditions for M4 are somewhat higher pressure and lower temperature than other two mixtures. With the increase of the evaporating pressure, the internal exergy destruction decreases.

Selected mixture reached relatively high values for both exergetic and thermal efficiency compared to other zeotropic mixtures; for instance, R-134a(0.7)/R-32(0.3) achieved thermal efficiency from 10.77% to 13.35% with the cycle high pressure of 7 MPa and temperatures of 393 K to 453 K and exergetic efficiencies of 38.57% in the same conditions (Chen et al., 2011). Our results also demonstrate certain advantages of using zeotropic mixtures over of pure components. The maximum thermal efficiency delivered by the pure component R-143a was 13.9% at turbine inlet pressure of 10 MPa and turbine inlet temperature of 470 K. This performance is 13% less than the maximum thermal efficiency developed by M3. The maximum exergetic efficiency delivered by the pure component R-143a was 44.3% at turbine inlet pressure of 3.8 MPa and turbine inlet temperature of 359 K. While the optimised cycle with the pure wet fluid can be powered using lower-grade heat source, its performance is 7.3% and 5.8% lower than the maximum exergetic efficiency developed by M1 and M3, respectively. Pure isentropic fluid may reach higher thermal efficiency than any of the mixtures; however, exergetic behaviour is significantly worse. Performance of the dry fluid R-C318 is also poorer at the same operational parameters.

In addition, in the interest of simplifying the quantitative analysis, calculated values were expressed using exergy destruction factor (EDF), the ratio between the exergy destruction in

each component and the net power generated by the system. EDF performance of the six mixtures at their optimal cycle parameters (those that correspond to the maximum exergy efficiency) is presented in Figure 9. In order to assess the effect of varying composition and nature of the other component in zeotropic mixtures, we have included the results for the pure R-143a, the common component in both types of tested mixtures. The distribution of irreversibilities in the different elements of the cycle is demonstrated by EDF value in each component. Naturally, the evaporator gives the highest contribution to the overall exergy destruction. One of the reasons for high irreversibility generated in the boiler is due to the large differences in temperatures between the states 2 and 3. EDF for the evaporator was found to be lower for pure R-143a than for any of the mixtures. However, the opposite was observed in all the other components of the cycle. For both types of zeotropic mixtures high EDF during heat-exchanges were found for intermediate mixing ratios. EDF values for isobaric transformations were generally greater for wet-dry fluid combination, R-143a/R-C318, compared to wet-isentropic mixtures, R-143a/R-124. Additionally, EDF for the turbine and the pump decreased for both types of mixtures as the concentration of R-143a was lowered.

Trends described above can be directly related to the glide temperature variations. According to these results, the temperature matching between the heat source and the working fluid in the boiler is of crucial importance and offers room for improvement. In general, as the pressure increases the exergy destroyed in the turbine and pump rise, whereas the exergy destroyed in the condenser and boiler decrease when compared for the same temperatures (El-Emam and Dincer, 2013). When the high pressure is kept constant, the exergy destroyed in each cycle component increases as the temperature is elevated with one exception being the pump, as its initial state is fixed and not a function of the heat source temperature. The condenser and boiler

benefit from increasing the high pressure, because the superheat is reduced and, consequently, the difference in the entropy between the two states decreases. As expected the total exergy destroyed follows the same pattern as the exergy destroyed in the boiler, as this component that dominates the total exergy destruction (Figure 8). From Figure 9 we gain insight that the exergy destroyed in the condenser is lower than for the pure R-143a component. For most zeotropic mixtures exergy destruction rate in the condenser was not comparable to exergy loss in the evaporator; it was even lower than that of the turbine. Use of zeotropic mixtures offers a better thermal match since the condensation process is non-isothermal and lower internal exergy destruction. However, the behaviour during the evaporation process does not offer the same advantage; the exergy destroyed in the boiler is greater for the zeotropic mixture than for the pure component.

Furthermore, we compared exergetic and energetic performance of each of the mixtures proposed under the optimised parameters for maximum thermal efficiency and maximum exergy efficiency, respectively. Exergetic behaviour appears to be in agreement with that observed in Figure 7: intermediate mixture compositions have lower efficiency. Similarly to results in Figure 4, R-143a/R-124 mixtures reached superior thermal efficiency, but at optimised exergetic parameters dissimilar trend is seen for R-143a/R-C318 mixtures. Thermal efficiency increases with the amount of dry fluid; however, this is due to lower optimal pressure and higher optimal temperature values for the maximum exergetic efficiency (Table 4). Nevertheless, thermal efficiency values are still higher than those reported in the literature for other zeotropic mixtures at similar conditions (Chys et al., 2012, Yang et al., 2013). These results reconfirm the nature and the mixing ratio of the fluids chosen for M3 are promising and the

prospect of employing this and similar zeotropic mixtures in low grade heat ORC should not be overlooked.

4. Conclusions

We report on the potential of zeotropic mixtures to be employed in supercritical Rankine cycle. Three different mole fractions of R-143a/R-124 and R-143a/R-C318 were studied and the quantitative analysis of the proposed working fluids has been carried out on the presumption that the basic cycle configuration is powered by a low energy heat source. The optimisation was conducted by varying the high pressure and temperature at the turbine inlet in order to identify the best thermal and exergetic performance.

The wet-dry fluid combination showed a great difference in terms of thermal efficiency compared to wet-isentropic mixtures. The former group achieved better performance, peaking at 16% for M3 (R-143a(0.2)/R-124(0.8)) at the maximum tested pressure and temperature, 10 MPa and 470 K, respectively. On the other hand, the exergetic analysis of the system showed a different trend; while the thermal efficiency varied proportionally with the amount of second component of mixture, differently though for each group of mixtures, the exergy efficiency appeared to fluctuate randomly for different mixing ratios. Four of the mixtures proposed are in the same range of exergetic efficiency (from 46.5% to 47.8%); M5 and M6 reached the lowest exergy efficiency with 41.6% and 43.9%, respectively, and the parameters for these optimised values are the minimal pressure and temperature values.

The common pure component, R-143a, showed 7.3% and 5.76% lower exergy efficiency compared to M1 and M3, respectively. Similarly, thermal efficiency of the cycle based on the pure component was generally found to be lower than any of the zeotropic mixtures. Our results identified M3 as the optimal selection of the zeotropic mixtures studied, which developed the best performance working with both sets of optimised parameters (maximum thermal/exergy efficiency). Further analysis is necessary to understand more in-depth behaviour of these mixtures under different operational parameters and in more complex cycle configurations. Moreover, R-143a/R-124 combination can be used a promising starting point for improvement of existing working fluids in supercritical Rankine cycle.

5. References

ANGELINO, G. & COLONNA DI PALIANO, P. 1998. Multicomponent Working Fluids For Organic Rankine Cycles (ORCs). *Energy,* 23**,** 449-463.

BAO, J. & ZHAO, L. 2013. A review of working fluid and expander selections for organic Rankine cycle. *Renewable and Sustainable Energy Reviews,* 24**,** 325-342.

CHEN, H., GOSWAMI, D. Y., RAHMAN, M. M. & STEFANAKOS, E. K. 2011. A supercritical Rankine cycle using zeotropic mixture working fluids for the conversion of low-grade heat into power. *Energy,* 36**,** 549-555.

CHEN, H., GOSWAMI, D. Y. & STEFANAKOS, E. K. 2010. A review of thermodynamic cycles and working fluids for the conversion of low-grade heat. *Renewable and Sustainable Energy Reviews,* 14**,** 3059-3067.

CHYS, M., VAN DEN BROEK, M., VANSLAMBROUCK, B. & DE PAEPE, M. 2012. Potential of zeotropic mixtures as working fluids in organic Rankine cycles. *Energy,* 44**,** 623-632.

DONG, B., XU, G., CAI, Y. & LI, H. 2014. Analysis of zeotropic mixtures used in high-temperature Organic Rankine cycle. *Energy Conversion and Management,* 84**,** 253-260.

EL-EMAM, R. S. & DINCER, I. 2013. Exergy and exergoeconomic analyses and optimization of geothermal organic Rankine cycle. *Applied Thermal Engineering,* 59**,** 435-444.

HEBERLE, F., PREIßINGER, M. & BRÜGGEMANN, D. 2012. Zeotropic mixtures as working fluids in Organic Rankine Cycles for low-enthalpy geothermal resources. *Renewable Energy,* 37**,** 364-370.

HIPÓLITO-VALENCIA, B. J., RUBIO-CASTRO, E., PONCE-ORTEGA, J. M., SERNA-GONZÁLEZ, M., NÁPOLES-RIVERA, F. & EL-HALWAGI, M. M. 2013. Optimal integration of organic Rankine cycles with industrial processes. *Energy Conversion and Management,* 73**,** 285-302.

KARELLAS, S. & SCHUSTER, A. 2008. Supercritical fluid parameters in organic Rankine cycle applications. *International Journal of Thermodynamics,* 11**,** 101-108.

KAŞKA, Ö. 2014. Energy and exergy analysis of an organic Rankine for power generation from waste heat recovery in steel industry. *Energy Conversion and Management,* 77**,** 108-117.

PAPADOPOULOS, A. I., STIJEPOVIC, M. & LINKE, P. 2010. On the systematic design and selection of optimal working fluids for Organic Rankine Cycles. *Applied Thermal Engineering,* 30**,** 760-769.

RADERMACHER, R. & HWANG, Y. 2005. *Vapor compression heat pumps with refrigerant mixtures*, CRC Press.

SALEH, B., KOGLBAUER, G., WENDLAND, M. & FISCHER, J. 2007. Working fluids for low-temperature organic Rankine cycles. *Energy,* 32**,** 1210-1221.

SCHUSTER, A., KARELLAS, S. & AUMANN, R. 2010. Efficiency optimization potential in supercritical Organic Rankine Cycles. *Energy,* 35**,** 1033-1039.

SHENGJUN, Z., HUAIXIN, W. & TAO, G. 2011. Performance comparison and parametric optimization of subcritical Organic Rankine Cycle (ORC) and transcritical power cycle system for low-temperature geothermal power generation. *Applied Energy,* 88**,** 2740-2754.

TCHANCHE, B. F., PAPADAKIS, G., LAMBRINOS, G. & FRANGOUDAKIS, A. 2009. Fluid selection for a low-temperature solar organic Rankine cycle. *Applied Thermal Engineering,* 29**,** 2468-2476.

WANG, X., LIU, X. & ZHANG, C. 2014. Parametric optimization and range analysis of Organic Rankine Cycle for binary-cycle geothermal plant. *Energy Conversion and Management,* 80**,** 256-265.

WANG, X. D. & ZHAO, L. 2009. Analysis of zeotropic mixtures used in low-temperature solar Rankine cycles for power generation. *Solar Energy,* 83**,** 605-613.

YANG, K., ZHANG, H., WANG, Z., ZHANG, J., YANG, F., WANG, E. & YAO, B. 2013. Study of zeotropic mixtures of ORC (organic Rankine cycle) under engine various operating conditions. *Energy,* 58**,** 494-510.

ZHAO, L. & BAO, J. 2014. The influence of composition shift on organic Rankine cycle (ORC) with zeotropic mixtures. *Energy Conversion and Management,* 83**,** 203-211.

Figure 1

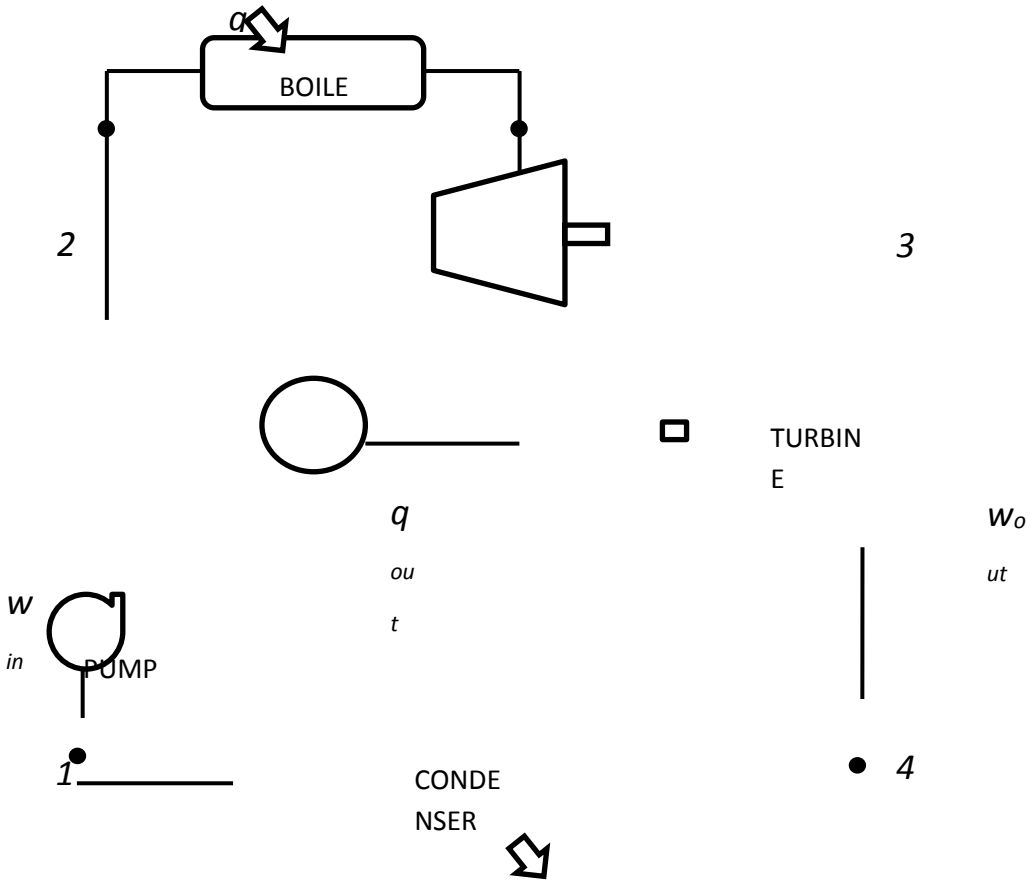

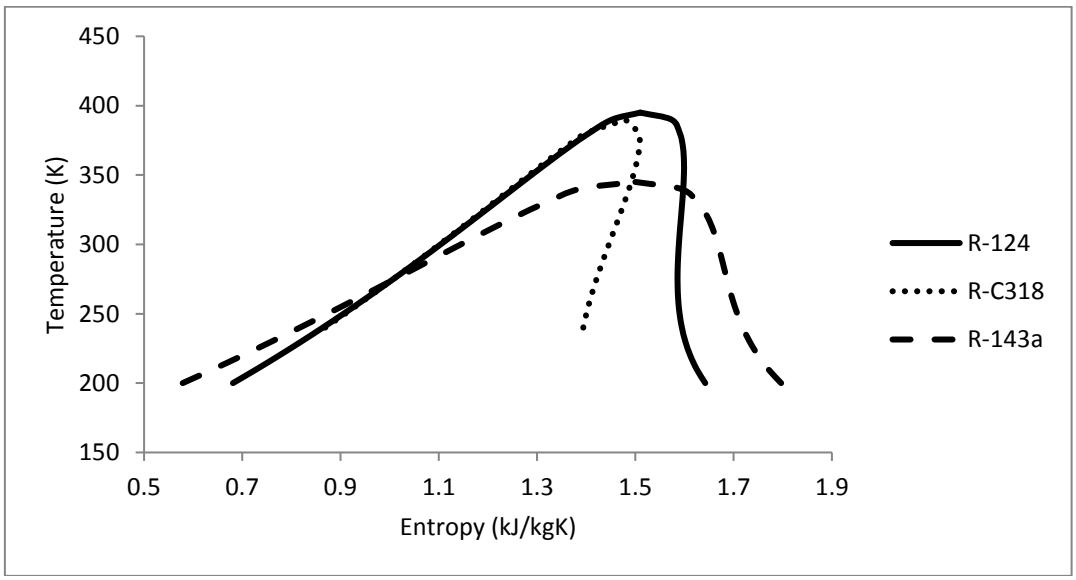

Figure 1. Cycle configuration (a); and *T-s* diagram (b) of dry R-C318 (dotted line), isentropic R-124 (dashed line) and wet R-143a fluids (solid line) used to form zeotropic mixtures

Figure 2

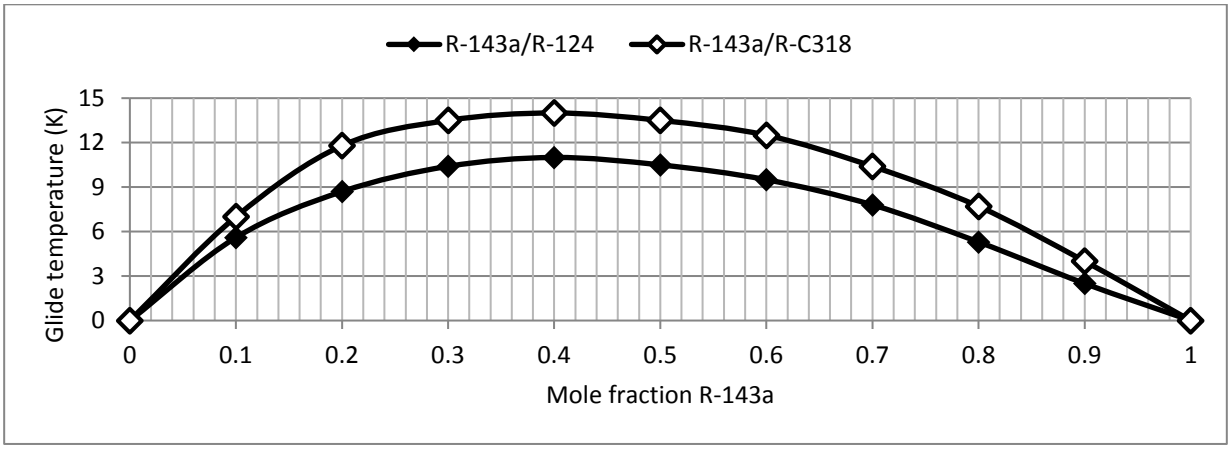

Figure 2. Temperature glide as a function of the composition of the zeotropic mixture: (♦), R-143a/R-124; (◊), R-143a/R-C318.

Figure 3

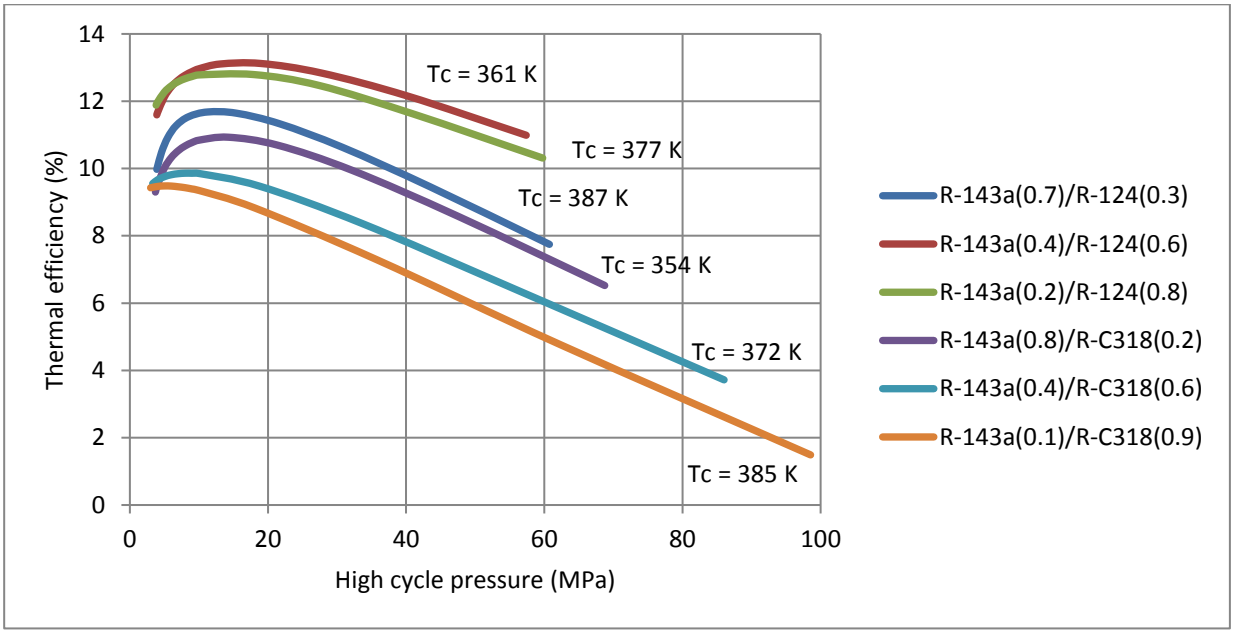

Figure 3. Effect of the high pressure level on thermal efficiency of SRC for selected zeotropic mixtures.

Figure 4

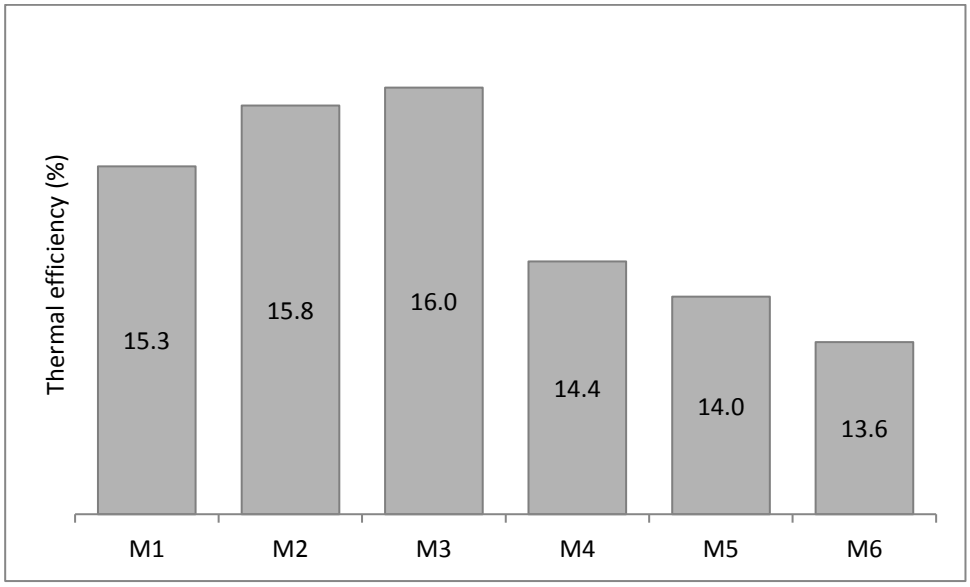

Figure 4. Highest achieved thermal efficiency of different zeotropic mixtures.

Figure 5

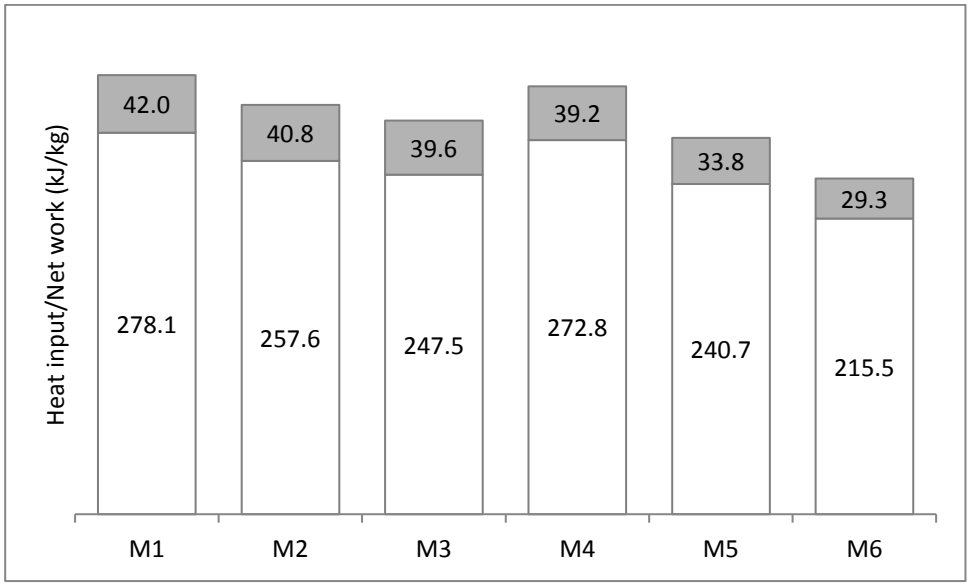

Figure 5. Heat input (white; kJ/kg) and net work (grey; kJ/kg) for the best thermal performance of the six zeotropic mixtures tested.

Figure 6

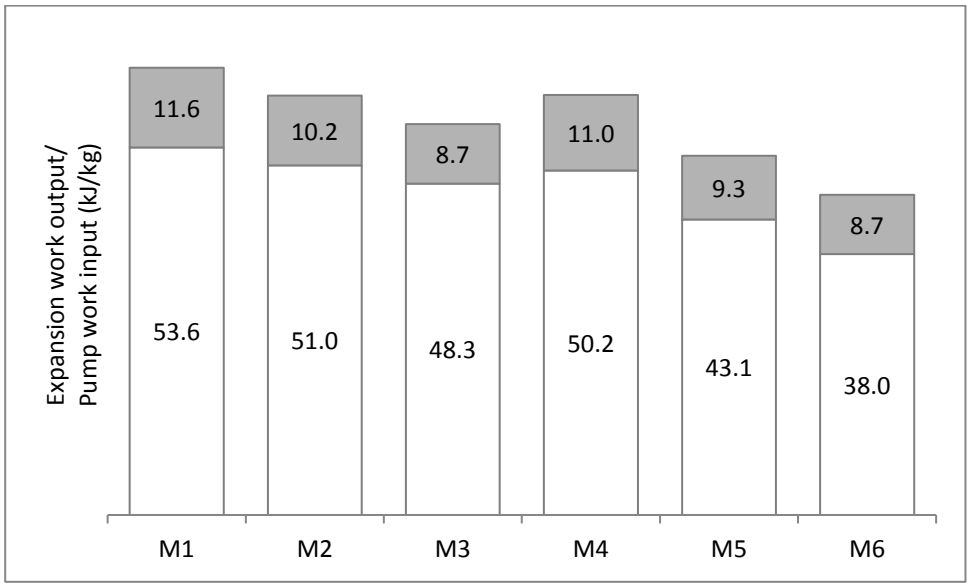

Figure 6. Expansion work output (white; kJ/kg) and pump work input (grey; kJ/kg) for the best thermal performance of the six zeotropic mixtures tested.

583 **Figure 7**

584

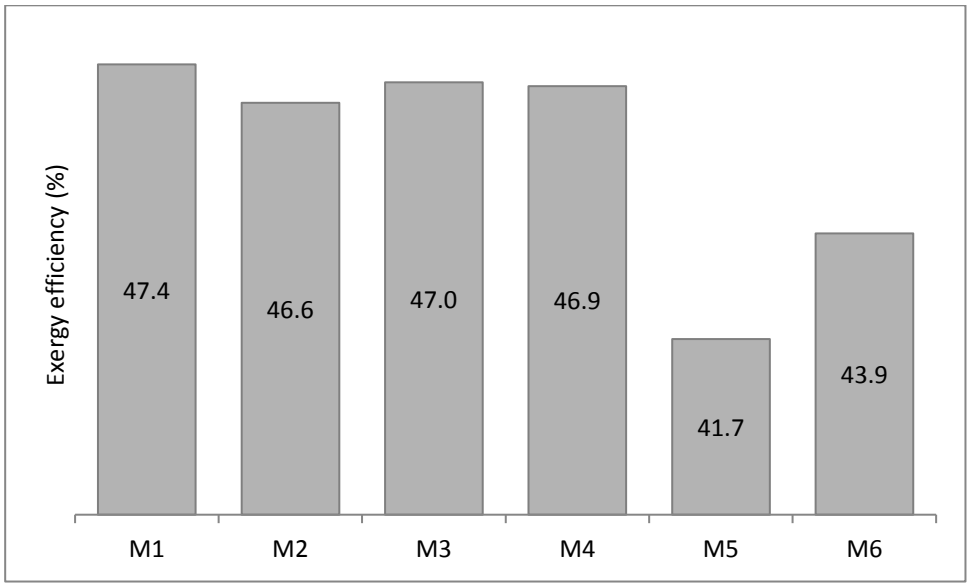

585

586

587 **Figure 7.** Highest achieved exergy efficiency of different zeotropic mixtures.

588

589

590

591

592

593

594

595

596

597

598

599

600

601

602

603

Figure 8

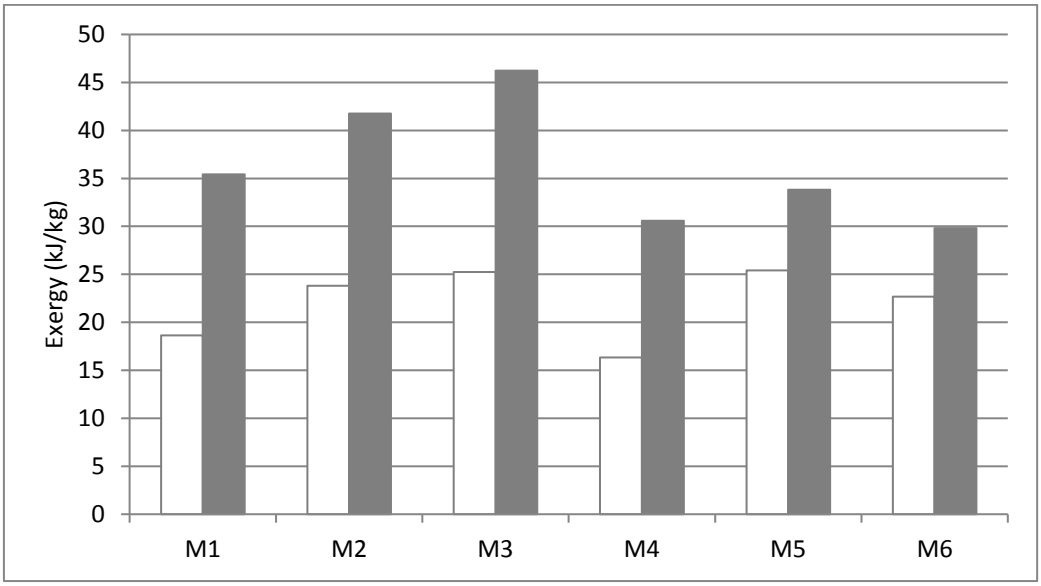

Figure 8. Total exergy destroyed (white) and heat source exergy (grey) for the best exergetic performance of the six zeotropic mixtures.

626 **Figure 9**

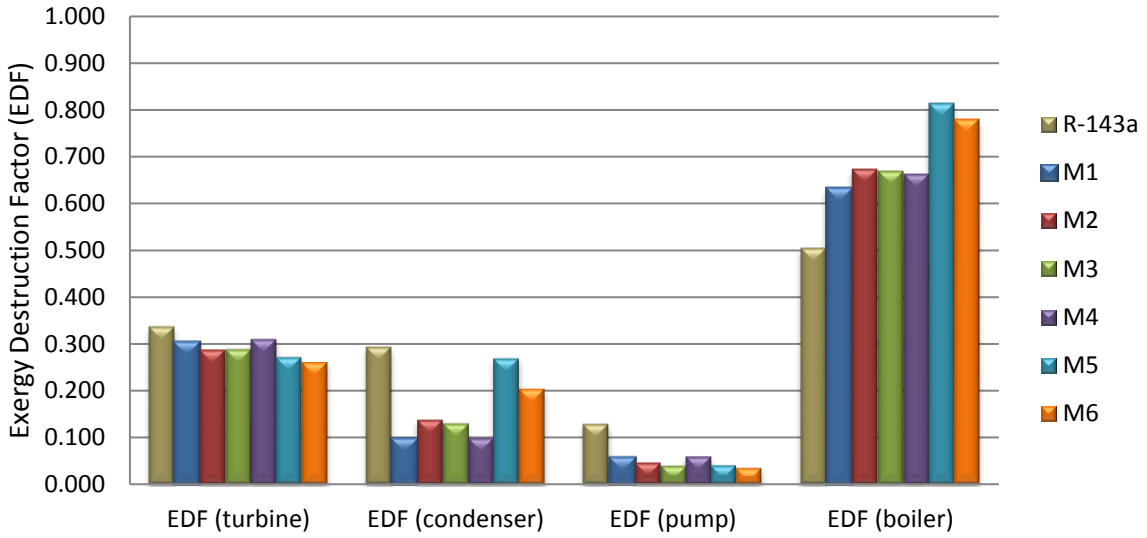

627

628 **Figure 9.** EDF of the zeotropic mixtures, evaluated for the best exergetic performance.

629

630

631

632

633

634

635

636

637

638

639

640

641

642

643

644

645

646

Figure 10

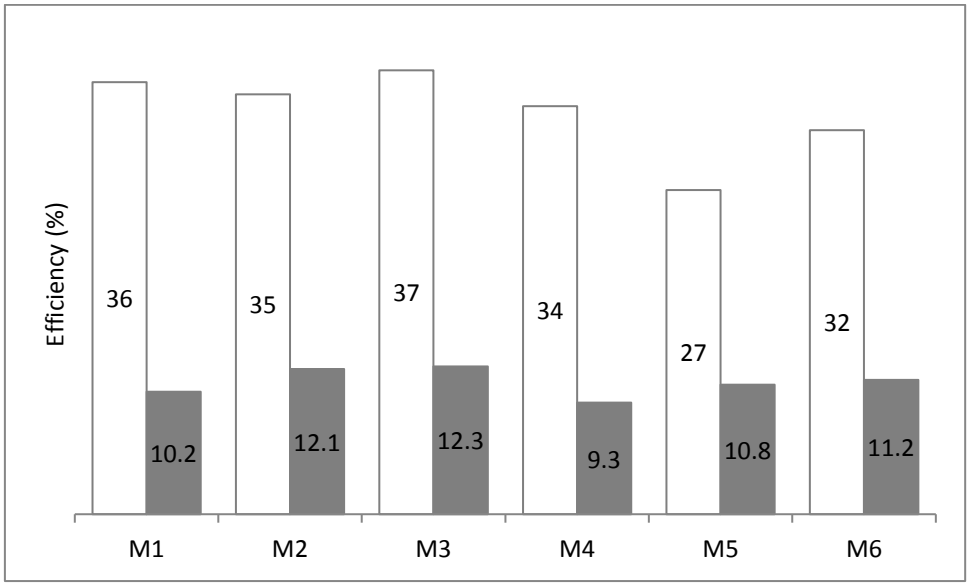

Figure 10. Performance comparison between two sets of cycle parameters: exergy efficiency calculated for max thermal efficiency parameters (white) and thermal efficiency calculated for max exergy efficiency parameters (grey).

Table1. Cycle process standard conditions

Parameters	
ΔT between working and cooling fluid at the condenser entrance	10°C
ΔT between working and source fluid at the boiler entrance	10°C
Inlet temperature of the cooling fluid (air)	15°C
Isentropic efficiency of feed pump	0.75
Isentropic efficiency of turbine	0.80
Minimum vapour quality at the turbine exit	90%

Table 2. Composition of six zeotropic mixtures in mole fractions.

Zeotropic Mixture	**R-143a**	**R-124**
M1	0.7	0.3
M2	0.4	0.6
M3	0.2	0.8
Zeotropic Mixture	**R-143a**	**R-C318**
M4	0.8	0.2
M5	0.4	0.6
M6	0.1	0.9

Table 3. Critical pressure and temperature and condensation conditions for the mixtures and composition studied.

Mixture	Composition	P_c (MPa)	T_c (K)	$P_{sat.vap}$ (MPa)
R-143a/R-124	0.7/0.3	3.9	361.4	0.8180
	0.4/0.6	3.9	377.0	0.5595
	0.2/0.8	3.8	386.8	0.4545
R-143a/R-C318	0.8/0.2	3.7	354.4	0.8670
	0.4/0.6	3.3	371.9	0.4719
	0.1/0.9	3.0	384.6	0.3409

760 **Table 4.** Overview of the optimised parameters for each mixture analysed.

Mixture	Thermal efficiency		Exergy efficiency	
	Maximum (%)	P & T (MPa & K)	Maximum (%)	P & T (MPa & K)
M1	15.26	10.0 & 470	47.79	3.9 & 368.8
M2	15.83	9.9 & 470	46.58	3.9 & 387.4
M3	16.00	9.0 & 470	47.01	3.8 & 389.6
M4	14.37	10.0 & 470	46.93	3.7 & 361.2
M5	14.04	10.0 & 470	41.66	3.3 & 379.0
M6	13.61	9.6 & 470	43.86	3.0 & 388.4

761

762